Journal of Molecular Catalysis A: Chemical 341 (2011) 42–50

Contents lists available at ScienceDirect

Journal of Molecular Catalysis A: Chemical

journal homepage: www.elsevier.com/locate/molcata

# The influence of ZnO, $CeO_2$ and $ZrO_2$ on nanoparticle-oxide-supported palladium oxide catalysts for the oxidative coupling of 4-methylpyridine

Justin J. Dodson, Luke M. Neal, Helena E. Hagelin-Weaver*

*University of Florida, Department of Chemical Engineering, P.O. Box 116005, Gainesville, FL 32611, United States*

ARTICLE INFO

*Article history:*
Received 22 December 2010
Received in revised form 8 March 2011
Accepted 27 March 2011
Available online 6 April 2011

*Keywords:*
Palladium oxide
$CeO_2$
$ZrO_2$ and ZnO additive oxides
Nanoparticle oxide supports
4-Methylpyridine
Aromatic coupling

ABSTRACT

4,4′-Dimethyl-2,2′-bipyridine is a useful but expensive chelating agent. Having more efficient routes to the synthesis of this compound would be advantageous to the wide-spread use of this fine chemical. In this work, the effects of adding strongly interacting oxides (ZnO, $CeO_2$, and $ZrO_2$) to PdO catalysts supported on high surface area n-$Al_2O_3$(+), n-MgO, and n-$TiO_2$ prepared via co- and sequential precipitation were investigated. The product yields obtained from these catalysts in the oxidative coupling of 4-methylpyridine are dependent on the additive, the support, and preparation method. Evidently, these are complex catalytic systems in that the PdO–additive and PdO–support interactions must be right to promote product formation while preventing palladium leaching and support or additive migration over the active Pd/PdO sites. Although PdO/n-ZnO catalysts are reasonably active in the coupling reaction, ZnO addition to PdO catalysts supported on n-$Al_2O_3$(+), n-MgO, or n-$TiO_2$ does not increase the yield in any case. $CeO_2$ and $ZrO_2$ can increase the product yields in the reaction depending on the support used. Due to strong PdO–$CeO_2$ interactions, the addition of $CeO_2$ in some cases results in $CeO_x$-migration and coverage of active PdO species or disrupts favorable PdO–support interactions leading to Pd leaching. Therefore, $ZrO_2$ is the better additive with co-precipitated PdO/$ZrO_2$/n-$Al_2O_3$(+) consistently producing yields in excess of $3.4 \pm 0.1$ g/g catalyst which is 36% higher than the $2.5 \pm 0.16$ g/g catalyst obtained from the PdO/n-$Al_2O_3$(+) (5 wt% Pd), the best catalyst previously reported for this reaction.



## 1. Introduction

Bipyridines possess the ability to coordinate to transition metal cations and form complexes with distinct photochemical and catalytic properties [1–4]. Bipyridine complexes with ruthenium are especially interesting in applications for organic light-emitting diodes [1] and chemiluminescence detection systems [5–7]. Various catalyst systems also use transition metal complexes with bipyridine ligands [8,9], including oxidative carbonylation [10], the Kumada-Corriu reaction [11], and the Suzuki cross-coupling reaction [12]. Yet, a widespread, large-scale usage is, in part, limited by the cost associated with bipyridine compounds. For instance, the price of 4,4′-dimethyl-2,2′-bipyridine exceeds $5,600 per kilogram [13]. Therefore, finding a more economical synthesis pathway for bipyridines is desirable. Environmental impacts are also an important concern. Hence, reactions with no solvents and no halogenated compounds are preferred.

The oxidative coupling of 4-methylpyridine to 4,4′-dimethyl-2,2′-bipyridine over palladium is a simple one-step process that uses neither solvents nor halogenated precursors (Scheme 1) with water and terpyridine as the only observed by-products. While this is an environmentally friendly process, the reaction rate is slow, and the catalyst undergoes deactivation which in turn limits the product yield [14]. Early research for this reaction focused on using palladium on carbon (Pd/C) catalysts with yields for 5 wt% and 10 wt% Pd loadings varying between 1.5 and 2.0 g bipyridine per g catalyst [14–17]. In our previous research, it was shown that both 5 wt% and 10 wt% palladium (metal basis) precipitated onto nanoparticle alumina [PdO/n-$Al_2O_3$(+)] yield approximately 2.5 g product per g catalyst [18]. As the product yield per gram of palladium for the catalyst with 5% palladium loading is almost twice that of the catalyst with 10% palladium loading, the 5 wt% palladium catalyst is more economical and is the best performing palladium catalyst reported to date [18,19]. Several other oxide supports including porous titania (p-$TiO_2$) and nanoparticle magnesia (n-MgO) with a 5 wt% palladium loading produce reasonable yields, similar to or higher than those obtained from a Pd/C catalyst [19]. In addition, catalysts supported on nanoparticle ceria (n-$CeO_2$), nanoparticle zinc oxide (n-ZnO), and nanoparticle zirconia (n-$ZrO_2$) were found to produce moderate yields (>1.5 g per g catalyst) despite relatively low support surface areas (<70 $m^2$/g) [19]. The moderate yields and high dispersions on the latter nanoparticle oxides indicate favorable metal–support interactions [19]. XPS confirms strong palladium–support interactions, as the Pd 3d peaks are

* Corresponding author. Tel.: +1 352 392 6585; fax: +1 352 392 9513.
*E-mail address:* hweaver@che.ufl.edu (H.E. Hagelin-Weaver).

1381-1169/$ – see front matter © 2011 Elsevier B.V. All rights reserved.
doi:10.1016/j.molcata.2011.03.022

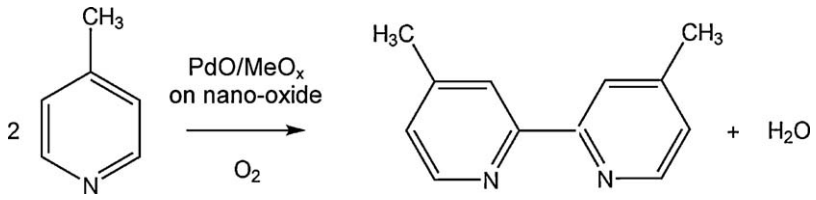


**Scheme 1.** Oxidative coupling of 4-methylpyridine over $PdO/MeO_x$/nano-oxide catalysts. $MeO_x$: ZnO, $CeO_2$ or $ZrO_2$. Nano-oxide: $Al_2O_3$(+), n-MgO or n-$TiO_2$.

shifted to higher binding energies indicating electron deficient PdO species on the surface [20]. The favorable interactions are further evidenced by the large number of studies on palladium promoted with or supported on $CeO_2$ [3,4,6,21–25], $ZrO_2$ [26,27] and Zn/ZnO [1,28–30]. These oxides are therefore potential promoters for palladium in the oxidative coupling of 4-methylpyridine. As it has been shown previously that the PdO on the surface of the catalysts is reduced to Pd metal after reaction, the reactions are likely limited by the reoxidation of palladium [14,20,31]. Consequently, the oxygen mobility and storage capacities of $CeO_2$ and $ZrO_2$ are particularly interesting for the oxidative coupling reaction. Assistance in oxygen transfer between palladium and the support could potentially produce highly effective catalysts.

In this study, the effects of ZnO, $CeO_2$ and $ZrO_2$ on a few selected nanoparticle oxide-supported catalysts were investigated. The n-$Al_2O_3$(+), n-$TiO_2$ and n-MgO supports were selected due to very high surface areas (>500 $m^2$/g) and, consequently, a strong potential for producing catalysts with high palladium dispersions. The additives were deposited on the support using two methods, (1) along with the active metal (co-precipitation) or (2) before the active metal (in a two-step sequential precipitation method). The main objectives of the study were to determine (1) if $CeO_2$, $ZrO_2$ and ZnO can promote palladium catalysts supported on n-$Al_2O_3$(+), n-$TiO_2$ and n-MgO, (2) if the effects of the additive are dependent on the nanoparticle oxide support used, (3) which is the more effective preparation method, co- or sequential precipitation of the additive and palladium, and (4) if a catalyst with a greater activity than the best to date, i.e. the PdO/n-$Al_2O_3$(+), can be prepared by adding one of these oxides.

## 2. Experimental

### 2.1. Catalyst preparation

The catalysts were prepared using commercially available nanoparticles, n-$Al_2O_3$(+), n-MgO and n-$TiO_2$, supplied by NanoScale Corporation [32] (Table 1). A precipitation method was used to deposit palladium and additive onto the supports. Using this method, aqueous solutions of metal nitrate(s) ($Pd(NO_3)_2{\cdot}2H_2O$: Fluka, $Ce(NO_3)_3{\cdot}6H_2O$: Sigma–Aldrich, $Zn(NO_3)_2{\cdot}6H_2O$: Alfa Aesar, and $ZrO(NO_3)_2{\cdot}6H_2O$: Sigma–Aldrich) were added to an aqueous dispersion of the support (either n-$Al_2O_3$(+), n-MgO or n-$TiO_2$). The mixture was titrated with sodium hydroxide to form metal hydroxide(s) on the support [33]. The amount of NaOH corresponded to a 50% stoichiometric excess, based on the amount of metal nitrate(s) used. The resulting mixture was aged overnight at room temperature before being filtered. The filtered material was rinsed in deionized water overnight and filtered again. The material was then dried at 105 °C overnight and calcined in air at 350 °C for 3 h.

All of the catalysts had loadings of 5% palladium and 5% additive by weight on a metal basis, unless otherwise noted. Two different precipitation methods were used; co-precipitation and sequential precipitation, to determine the effects of the additive. For the co-precipitation method, cerium nitrate, zinc nitrate or zirconium nitrate was dissolved with palladium nitrate in deionized water before being added to an aqueous dispersion of the support. The metals were then precipitated together onto the support by titration with a sodium hydroxide solution. In the sequential precipitation method, the metal oxide additive was deposited first by precipitation onto the support, aged, rinsed, dried and calcined before repeating the process to deposit the palladium.

### 2.2. Reaction conditions

The reactant, 4-methylpyridine (Acros), was doubly distilled over KOH prior to use. In a typical reaction run, 0.7 g of catalyst was placed in a round bottom flask with 7 g of the distilled 4-methylpyridine. The reaction mixture was evacuated followed by the introduction of an oxygen atmosphere. The mixture was then heated to the boiling point (145 °C) under continuous agitation. After refluxing for 72 h, the flask contents were filtered using a glass micro-fiber filter and washed with chloroform to dissolve the product. The product was obtained by removing the chloroform, water, and unreacted 4-methylpyridine using a rotary evaporator.

### 2.3. Catalyst characterization

The as received support surface areas and the surface areas of the prepared catalyst were determined by multipoint Brunauer–Emmett–Teller (BET) isotherms on a Quantachrome Nova 1200 instrument as described in previous work [18].

Chemisorption measurements were performed in a Quantachrome ChemBET 3000 instrument and used to characterize the active catalyst surface area. The catalysts were first reduced with hydrogen at 170 °C for 1 h, and then outgassed in nitrogen at 170 °C for another hour. The mild reduction conditions were used to limit sintering of the Pd particles on the surface. This was followed by pulse titration with carbon monoxide to characterize the palladium dispersions of the catalysts. Detailed descriptions of the procedure and calculations are given in previous work [19]. While PdO is believed to be the active phase, or at least a necessary precursor, the CO chemisorption measurements on reduced catalysts are important since the PdO surface area cannot be measured directly. It is assumed that there is a correlation between the original PdO surface area and the Pd surface area of the reduced catalyst. Previous XRD and TEM data support this assumption [20,31].

The XRD data was gathered on a Philips powder X-ray diffractometer using Bragg–Brentano geometry with Cu Kα radiation (λ = 1.54 Å). Selected catalyst powders were secured onto a glass slide with double-sided sticky tape prior to measurements.

The thermogravimetric analysis (TGA) of the three nanoparticle supports was carried out on a Mettler Toledo TGA/SDTA (scanning differential thermal analysis) with sample weights between 4 and 20 mg, under a 40 mL $min^{-1}$ air flow. The samples were heated from room temperature to 105 °C at 20 °C $min^{-1}$ and held for 5 min before again being heated from 105 °C to 1000 °C at 10 °C $min^{-1}$.

## 3. Results

All prepared catalysts were subjected to activity measurements in the coupling reaction of 4-methylpyridine. The results are sum-

**Table 1**
Catalyst support properties.

| Support oxide | NanoScale Product[a] | SA ($m^2/g$)[b] | SA ($m^2/g$) after calcination[c] | $NH_3$ ($S\,cm^3/g$)[d] | $CO_2$ ($S\,cm^3/g$)[e] |
|---|---|---|---|---|---|
| n-$Al_2O_3$(+) | NanoActive Aluminum Oxide Plus | 695 | 515[f] | 9.0 | 0.75 |
| n-MgO | NanoActive Magnesium Oxide Plus | 685 | 616 | 3.4 | 2.0 |
| n-$TiO_2$ | NanoActive Titanium Dioxide | 505 | 133 | 4.0 | 0.6 |

[a] Nanoparticles purchased from NanoScale Corporation: http://www.nanoscalecorp.com/content.php/chemicals/powders/ accessed on 11/19/2010.
[b] BET surface area after drying at 105 °C for 3 h.
[c] BET surface area after calcination at 350 °C for 3 h.
[d] Adsorbed amount of $NH_3$ on support. Measured by pulse titration after outgassing in flowing nitrogen at 105 °C for 1 h [19].
[e] Adsorbed amount of $CO_2$ on support. Measured by pulse titration after outgassing in flowing nitrogen at 105 °C for 1 h [19].
[f] Surface area after calcination at 350 °C for 24 h.

marized in Table 2 and Fig. 1. The catalysts without additives from previous research, PdO/n-$Al_2O_3$(+), PdO/n-$TiO_2$, and PdO/n-MgO, as well as some additional catalysts prepared using a slightly modified preparation procedure, are included for comparison. The properties of the supports have been presented in a previous paper [19], but are summarized in Table 1 as they are important in the current study. As seen in Table 2, the effects of the additives are dependent on the identities of the additive and support as well as the preparation method.

To obtain more information about the effects of the oxide additives and the preparation methods on the different supports, the overall surface areas were determined, and CO chemisorption measurements were performed to estimate the Pd surface areas of the catalysts. The results from these measurements are presented in Table 3.

## 4. Discussion

### 4.1. PdO supported on nanoparticle alumina

Previous research showed that the PdO/n-$Al_2O_3$(+) catalyst is the most active and reproducible catalyst amongst the various catalysts examined for this reaction. Addition of ZnO, $CeO_2$ and $ZrO_2$ to this catalyst was investigated in an attempt to improve the product yields.

#### 4.1.1. Precalcination of n-$Al_2O_3$(+)

As Fig. 1 indicates, the sequential precipitation method is inferior to co-precipitation for catalysts supported on n-$Al_2O_3$(+). Thus, the effect of the first calcination treatment was explored. A n-$Al_2O_3$(+) sample was calcined in air at 350 °C for 3 h before palladium deposition and then tested for activity. This support pretreatment results in a significantly reduced product yield (Table 2). The difference between the catalysts prepared using heat-treated and untreated supports is attributable to the lower Pd surface area on the heat-treated n-$Al_2O_3$(+). The lower Pd surface area is not caused by a drastic reduction in support surface area, as the surface area of the n-$Al_2O_3$(+) is still above 500 $m^2/g$ even after calcination for 24 h at 350 °C.

Previous research revealed that n-$Al_2O_3$(+) mainly consists of poorly crystalline γ-AlO(OH) which transforms to γ-$Al_2O_3$ between 350 °C and 450 °C [31]. From TGA measurements (Fig. 2), it is evident that a significant fraction of the support's "dry" weight loss (weight lost after drying at 105 °C for 5 min) occurs between 105 °C

**Table 2**
Catalytic activities of prepared catalysts.

| Entry | Preparation method[a] | Support | Additive | Yield (g product/g catalyst) | Yield (g product/g Pd) |
|---|---|---|---|---|---|
| 1[b] | PT | n-$Al_2O_3$(+) | – | 2.5 | 50 |
| 2 | PT[c] | n-$Al_2O_3$(+) | – | 1.8 | 36 |
| 3 | CP | n-$Al_2O_3$(+) | ZnO | 2.4 | 47 |
| 4 | SQ | n-$Al_2O_3$(+) | ZnO | 1.6 | 30 |
| 5 | CP | n-$Al_2O_3$(+) | $CeO_2$ | 2.5 | 51 |
| 6 | SQ | n-$Al_2O_3$(+) | $CeO_2$ | 1.4 | 26 |
| 7 | CP | n-$Al_2O_3$(+) | $ZrO_2$ | 3.4 | 68 |
| 8 | SQ | n-$Al_2O_3$(+) | $ZrO_2$ | 2.5 | 49 |
| 9 | SQ[d] | n-$Al_2O_3$(+) | $ZrO_2$ | 3.3 | 66 |
| 10[b] | PT | n-MgO | – | 2.3 | 46 |
| 11 | PT[c] | n-MgO | – | 1.7 | 32 |
| 12 | CP | n-MgO | ZnO | 1.4 | 27 |
| 13 | SQ | n-MgO | ZnO | 0.9 | 18 |
| 14 | CP | n-MgO | $CeO_2$ | 2.2 | 43 |
| 15 | SQ | n-MgO | $CeO_2$ | 2.7 | 53 |
| 16 | SQ[d] | n-MgO | $CeO_2$ | 2.6 | 52 |
| 17 | CP | n-MgO | $ZrO_2$ | 2.1 | 43 |
| 18 | SQ | n-MgO | $ZrO_2$ | 1.8 | 37 |
| 19[b] | PT | n-$TiO_2$ | – | 1.6 | 31 |
| 20 | PT[c] | n-$TiO_2$ | – | 1.5 | 31 |
| 21 | CP | n-$TiO_2$ | ZnO | 1.1 | 23 |
| 22 | SQ | n-$TiO_2$ | ZnO | 1.2 | 24 |
| 23 | CP | n-$TiO_2$ | $CeO_2$ | 1.2 | 25 |
| 24 | SQ | n-$TiO_2$ | $CeO_2$ | 1.6 | 32 |
| 25 | CP | n-$TiO_2$ | $ZrO_2$ | 0.6 | 13 |
| 26 | SQ | n-$TiO_2$ | $ZrO_2$ | 1.9 | 37 |
| 27 | SQ[d] | n-$TiO_2$ | $ZrO_2$ | 2.0 | 41 |

[a] Preparation methods: PT, precipitation; CP, co-precipitation; SQ, sequential precipitation.
[b] Results from previous work [19].
[c] Catalyst prepared using a precalcined support.
[d] Catalyst prepared using a modified sequential precipitation, where the catalyst is simply filtered (not calcined) before the second deposition.

**Table 3**
Catalyst surface areas, CO adsorption, palladium dispersions and turnover numbers of prepared catalysts.

| Catalyst [5/5/90%][a] | Deposition method[b] | Surface area ($m^2$/g) | CO ads. (μL CO/g cat) | Dispersion (%) | Pd SA ($m^2$/g) | TON[c] |
|---|---|---|---|---|---|---|
| PdO/n-$Al_2O_3$(+)[d] | PT | 180 | 4600 | 44 | 9.7 | 66 |
| PdO/n-$Al_2O_3$(+) | PT[e] | 215 | 1800 | 17 | 3.8 | 120 |
| PdO/ZnO/n-$Al_2O_3$(+) | CP | 245 | 4490 | 43 | 9.5 | 64 |
| PdO/ZnO/n-$Al_2O_3$(+) | SQ | 235 | 2800 | 27 | 5.9 | 66 |
| PdO/$CeO_2$/n-$Al_2O_3$(+) | CP | 220 | 5380 | 51 | 11.4 | 57 |
| PdO/$CeO_2$/n-$Al_2O_3$(+) | SQ | 250 | 2960 | 28 | 6.3 | 54 |
| PdO/$ZrO_2$/n-$Al_2O_3$(+) | CP | 220 | 4830 | 46 | 10.2 | 85 |
| PdO/$ZrO_2$/n-$Al_2O_3$(+) | SQ | 215 | 1730 | 16 | 3.7 | 172 |
| PdO/$ZrO_2$/n-$Al_2O_3$(+) | SQ[f] | 214 | 3940 | 37 | 8.3 | 103 |
| PdO/n-MgO[d] | PT | 85 | 2350 | 22 | 5.0 | 119 |
| PdO/n-MgO | PT[e] | 101 | 2490 | 24 | 5.3 | 78 |
| PdO/ZnO/n-MgO | CP | 140 | 780 | 7 | 1.7 | 213 |
| PdO/ZnO/n-MgO | SQ | 50 | 1520 | 14 | 3.2 | 70 |
| PdO/$CeO_2$/n-MgO | CP | 64 | 2560 | 24 | 5.4 | 101 |
| PdO/$CeO_2$/n-MgO | SQ | 120 | 4190 | 40 | 8.9 | 77 |
| PdO/$CeO_2$/n-MgO | SQ[f] | 49 | 2290 | 22 | 4.8 | 137 |
| PdO/$ZrO_2$/n-MgO | CP | 165 | 3740 | 35 | 7.9 | 70 |
| PdO/$ZrO_2$/n-MgO | SQ | 125 | 3200 | 30 | 6.8 | 71 |
| PdO/n-$TiO_2$[d] | PT | 210 | 4150 | 39 | 8.8 | 46 |
| PdO/n-$TiO_2$ | PT[e] | 110 | 1720 | 16 | 3.6 | 110 |
| PdO/ZnO/n-$TiO_2$ | CP | 230 | 2870 | 27 | 6.1 | 48 |
| PdO/ZnO/n-$TiO_2$ | SQ | 190 | 4620 | 44 | 9.8 | 31 |
| PdO/$CeO_2$/n-$TiO_2$ | CP | 230 | 5050 | 48 | 10.7 | 30 |
| PdO/$CeO_2$/n-$TiO_2$ | SQ | 170 | 5030 | 48 | 10.7 | 39 |
| PdO/$ZrO_2$/n-$TiO_2$ | CP | 120 | 4860 | 46 | 10.3 | 16 |
| PdO/$ZrO_2$/n-$TiO_2$ | SQ | 110 | 5160 | 49 | 10.9 | 44 |
| PdO/$ZrO_2$/n-$TiO_2$ | SQ[f] | 186 | 5780 | 55 | 12.2 | 43 |

[a] [5/5/90]: Weight percent of different components. PdO and additive on metal basis and support on metal oxide basis.
[b] Preparation methods: PT, precipitation; CP, co-precipitation; SQ, sequential precipitation.
[c] TON = turnover number: number of product molecules formed per palladium surface atom.
[d] Results from previous work [19].
[e] Catalyst prepared using a precalcined support.
[f] Catalyst prepared using a modified sequential precipitation, where the catalyst is simply filtered (not calcined) before the second deposition.

and 350 °C. As roughly 4% out of the total 12% dry weight-loss is lost during the ramp to 350 °C (a 15% total weight loss would be expected for complete conversion of a 100% AlO(OH) to γ-$Al_2O_3$), a significant fraction of the AlO(OH) is expected to transform into γ-$Al_2O_3$ during the 3 h calcination at 350 °C. Even though the XRD spectra of catalysts calcined at 350 °C reveal only poorly crystalline AlO(OH) (and no γ-$Al_2O_3$), TGA strongly indicates that a significant fraction of the original AlO(OH) has decomposed after calcination at this temperature. The XRD measurements cannot detect the developing poorly crystalline γ-$Al_2O_3$ phase. The low Pd surface area measured on the catalysts prepared using the precalcined n-$Al_2O_3$(+) therefore supports our previous conclusion that the hydroxyl groups in the n-$Al_2O_3$(+) (or rather the n-AlO(OH)) support are important to obtain a high Pd surface area. It is our belief that these hydroxyl groups interact with the $Pd^{2+}$ ions during the precipitation process and thereby result in high Pd dispersions on these catalysts.

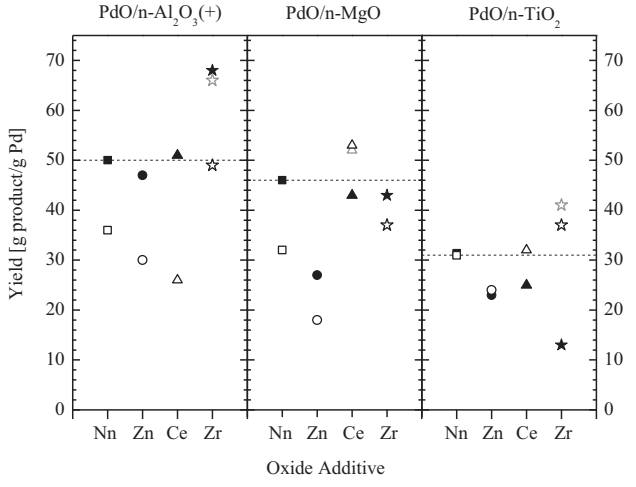


**Fig. 1.** Activity data from prepared catalysts. Nn = PdO/support only, no additive oxide. Additive oxide: Zn = ZnO, Ce = $CeO_2$, Zr = $ZrO_2$. Filled symbols are results from the co-precipitation method (Zn, Ce or Zr), as well as the precipitated reference PdO/support catalysts (Nn) and open symbols are results from the sequential precipitation method (Zn, Ce or Zr), or for PdO/support catalysts (no additive) prepared using a precalcined support (Nn). The open grey symbols are results from the modified sequential precipitation method (filtration only, no calcination).

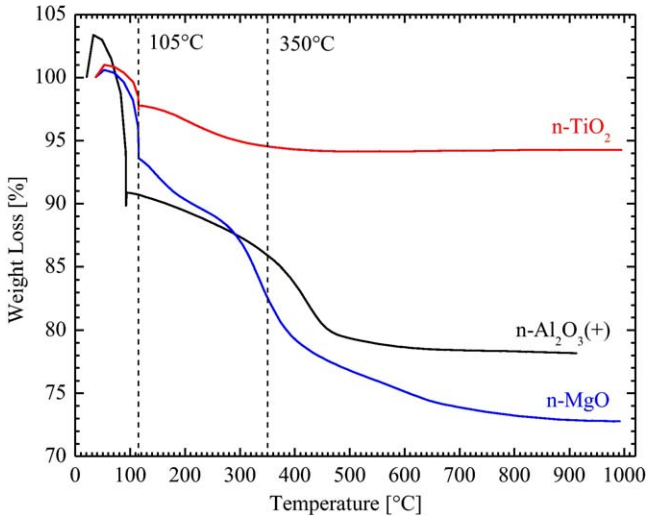


**Fig. 2.** Thermogravimetric analysis (TGA) data obtained from n-$TiO_2$ (red), n-$Al_2O_3$(+) (black) and n-MgO (blue) supports. Dashed lines mark the drying temperature (105 °C) and calcination temperature (350 °C). (For interpretation of the references to color in this figure legend, the reader is referred to the web version of the article.)

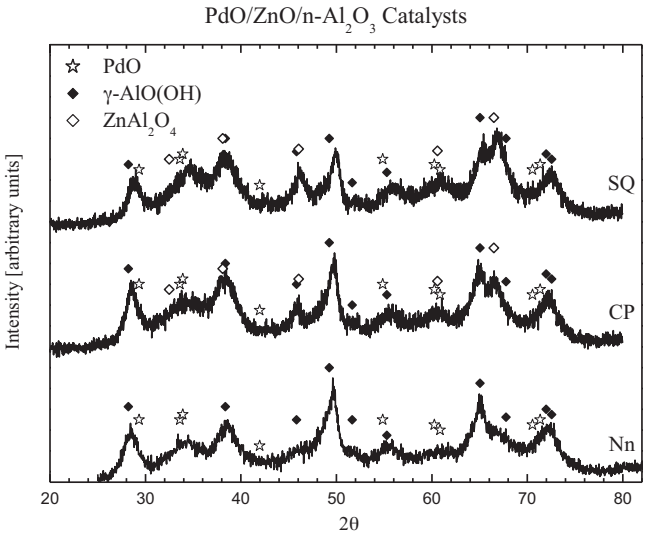


**Fig. 3.** X-ray diffraction (XRD) data obtained from PdO/ZnO/n-$Al_2O_3$(+) catalysts prepared using the co-precipitation (CP) and the sequential precipitation (SQ) methods, and PdO/n-$Al_2O_3$(+) catalyst with no added ZnO (Nn).

#### 4.1.2. ZnO addition

While ZnO has been shown to result in favorable Pd–Zn interactions in PdO/n-ZnO catalysts [28], adding ZnO to the PdO/n-$Al_2O_3$(+) catalyst does not have a positive effect on the product yield irrespective of catalyst preparation method used (Fig. 1 and Table 2). The co-precipitation of ZnO and PdO precursors only slightly decreases the yield, but the sequential precipitation method results in a significant decrease to half the original yield from PdO/n-$Al_2O_3$(+). This is even lower than the yield obtained from the PdO supported on precalcined n-$Al_2O_3$(+). Previous results have shown that deposition of ZnO onto n-$Al_2O_3$(+) support under similar preparation techniques results in facile $ZnAl_2O_4$ formation [34]. Therefore XRD spectra were obtained for co-precipitated (CP) and sequentially precipitated (SQ) PdO/ZnO/n-$Al_2O_3$(+) catalysts, and reveal additional peaks which are reasonably consistent with $ZnAl_2O_4$ (Fig. 3). The peaks due to $ZnAl_2O_4$ are more pronounced on the SQ catalyst indicating that the presence of palladium may disrupt the Zn–Al interactions during co-precipitation, possibly due to Pd–Zn interactions. The lower yields obtained from the ZnO-containing catalysts correlate with the reduction in Pd surface area, as both the CP and SQ catalysts' turnover numbers are not significantly lower than the PdO/n-$Al_2O_3$(+) catalyst without added ZnO. In the case of the sequentially prepared PdO/ZnO/n-$Al_2O_3$(+) catalyst, the lower Pd surface area is attributed to the smaller support surface area and the removal of the surface hydroxyl groups during ZnO addition and calcination. In the case of the CP catalyst, a slightly lower Pd surface area is observed, while the overall surface area is higher, compared to the PdO/n-$Al_2O_3$(+), which could be due to some ZnO covering the PdO on the surface.

#### 4.1.3. $CeO_2$ addition

Co-precipitation of $CeO_2$ and PdO precursors on the n-$Al_2O_3$(+) support does not affect the average product yield significantly, even though the measured Pd surface area does increase (Tables 2 and 3). As with the ZnO additive, the sequential addition of $CeO_2$ produces an inferior catalyst compared to the co-precipitated PdO/$CeO_2$/n-$Al_2O_3$(+) catalyst and gives a significantly lower yield than PdO supported on a precalcined n-$Al_2O_3$(+) support. One reason for the low yield is a lower Pd surface area for the SQ PdO/$CeO_2$/n-$Al_2O_3$(+) than the PdO/n-$Al_2O_3$(+) catalyst with no $CeO_2$ additive. However, as the Pd surface area of the SQ PdO/$CeO_2$/n-$Al_2O_3$(+) catalyst is higher than that of PdO supported on the precalcined n-$Al_2O_3$(+), the turnover number for the SQ catalyst is lower than expected from $CeO_2$-containing catalysts. Upon examining the results from the SQ PdO/$CeO_2$/n-$Al_2O_3$(+) catalyst series, the yields vary significantly from 2.1 to 3.1 (i.e. $2.6 \pm 0.44$) g product/g catalyst. As strong PdO–$CeO_2$ interactions leading to migration of $CeO_x$ over the palladium have been observed on these and other catalysts [20,35,36], the yield variation in this case may be due to varying degrees of $CeO_2$ coverage of Pd active sites. $CeO_2$ migration during reaction would explain the lower than expected yields despite the reasonably high Pd surface areas from the PdO/$CeO_2$/n-$Al_2O_3$(+) catalysts.

#### 4.1.4. $ZrO_2$ addition

In contrast to the ZnO and $CeO_2$, addition of $ZrO_2$ via the co-precipitation method consistently demonstrates a significant improvement in the catalyst performance compared to the PdO/n-$Al_2O_3$(+) catalyst. The co-precipitated method produces a yield of $3.4 \pm 0.1$ g/g catalyst, which is approximately a 36% increase over the highest yield reported to date for this reaction. As with the other oxides added to the PdO/n-$Al_2O_3$(+) catalyst, sequential precipitation results in an inferior catalyst. However, the yield from the SQ PdO/$ZrO_2$/n-$Al_2O_3$(+) catalyst is only slightly lower than that from the PdO/n-$Al_2O_3$(+) catalyst, and, more importantly, is significantly higher than the yield obtained from PdO on a precalcined n-$Al_2O_3$(+) support. This indicates that $ZrO_2$ is acting as a promoter for the PdO/n-$Al_2O_3$(+) catalyst regardless of the preparation method.

#### 4.1.5. Modified preparation method

To further investigate the differences between the co-precipitation and the sequential precipitation methods, the sequential precipitation procedure was modified for the PdO/$ZrO_2$/n-$Al_2O_3$(+) catalyst. Instead of calcining the catalyst after deposition of $ZrO_2$, one catalyst was simply aged, rinsed, and filtered before re-dispersion in an aqueous $Pd^{2+}$ solution for PdO deposition. This results in a catalyst with almost the same activity as a co-precipitated catalyst (Table 2, Entries 7 and 9) and confirms that the calcination step between depositions has an undesirable effect on the catalysts.

In summary, the co-precipitation method is preferred over the sequential precipitation on n-$Al_2O_3$(+)-supported palladium catalysts. The calcination step between depositions is detrimental and results in lower Pd surface areas which are attributed to removal of OH groups on the support. Only $ZrO_2$ is promoting the activity of a PdO/n-$Al_2O_3$(+) catalyst.

### 4.2. PdO supported on nanoparticle magnesia

While the n-MgO support has a surface area comparable to the n-$Al_2O_3$(+) support (>650 $m^2$/g), the PdO/n-MgO catalyst is not as active as the PdO/n-$Al_2O_3$(+) catalyst in the coupling of 4-methylpyridine, mainly due to a lower Pd surface area. The effects of ZnO, $CeO_2$ and $ZrO_2$ addition to the PdO/n-MgO catalyst were therefore investigated to determine if the yields of this MgO-supported PdO catalyst could be improved.

#### 4.2.1. Precalcination of n-MgO

The behavior of the PdO supported on the precalcined n-MgO is similar to that of PdO on precalcined n-$Al_2O_3$(+) as a significant reduction in product yield is observed (Fig. 1). However, in contrast to the PdO catalysts supported on n-$Al_2O_3$(+), the lower yield is not due to a decreased Pd surface area on the precalcined n-MgO support (Table 3). TGA analysis reveals that the n-MgO support exhibits a similar weight loss behavior upon heating as seen in the n-$Al_2O_3$(+) support (Fig. 2). This suggests that the n-MgO support consists of a significant amount of $Mg(OH)_2$. While most

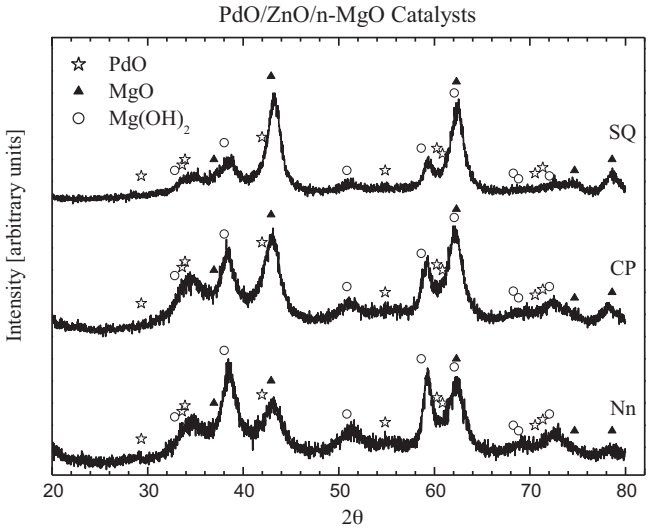


**Fig. 4.** X-ray diffraction (XRD) data obtained from PdO/ZnO/n-MgO catalysts prepared using the co-precipitation (CP) and the sequential precipitation (SQ) methods, and PdO/n-MgO catalyst with no added ZnO (Nn).

of the weight-loss in the AlO(OH)-containing n-$Al_2O_3$(+) support occurs in the temperature range between 350 °C and 450 °C, the n-MgO support loses weight over the whole temperature range from 100 °C to 800 °C, although a very rapid weight-loss between 300 °C and 400 °C is observed. The total weight-loss on a dry basis is 21% (i.e. the weight lost after the drying period). As a total weight-loss of 31% is expected for converting a sample consisting of 100% $Mg(OH)_2$ to MgO, the TGA measurements indicate that approximately 70% of the n-MgO is $Mg(OH)_2$. It is expected that a significant fraction of the $Mg(OH)_2$ remains in the sample after calcination at 350 °C for 3 h. This is consistent with an XRD spectrum obtained from the PdO/n-MgO catalyst after calcination, which reveals peaks from both MgO and $Mg(OH)_2$ (Fig. 4). Consequently, after precalcination, a large number of hydroxyl groups are likely still present, which can interact with the $Pd^{2+}$ ions during deposition to yield a high Pd dispersion. Despite similar initial support surfaces areas, the Pd surface area is not as high on the n-MgO as the n-$Al_2O_3$(+) support, which may be due to more acidic hydroxyl groups on the alumina support compared with the basic magnesia support (Table 1).

#### 4.2.2. ZnO addition

Similar to the n-$Al_2O_3$(+)-supported catalysts, addition of ZnO to the PdO/n-MgO catalyst results in a significant reduction in the product yield irrespective of the preparation method. As expected from the results over the PdO supported on precalcined n-MgO, the sequential precipitation method is inferior to the co-precipitation method. The lower yields obtained from the PdO/ZnO/n-MgO catalysts are largely attributed to the lower Pd surface area compared to the PdO/n-MgO catalyst with no added ZnO. The larger overall surface area and the smaller Pd surface area of the CP compared to the SQ PdO/ZnO/n-MgO catalyst indicates more ZnO covering the surface PdO during co-precipitation. Despite the lower Pd surface area of the CP PdO/ZnO/n-MgO catalyst, the product yield is higher than that obtained from the SQ catalyst, resulting in a higher CP catalyst turnover number (Table 3). Thus, the palladium on the surface of the CP PdO/ZnO/n-MgO catalyst is more active, or at least more stable (*vide infra*), than on the SQ catalyst.

According to XRD the main differences between the SQ and the CP PdO/ZnO/n-MgO catalysts appear to be (1) a more crystalline PdO on the CP PdO/ZnO/n-MgO catalyst and (2) less $Mg(OH)_2$ on the SQ PdO/ZnO/n-MgO catalyst (Fig. 4). A lower $Mg(OH)_2$ content in the SQ PdO/ZnO/n-MgO catalyst is expected with the second calcination. While no other crystal phases are visible in the XRD spectra, the formation of poorly crystalline mixed oxides between ZnO and n-MgO ($Mg_xZn_{1-x}O$) [37] on this catalyst surface cannot be excluded. Strong interactions between ZnO and n-MgO could disrupt favorable palladium–support or Pd–ZnO interactions leading to low Pd surface areas and catalytic activities.

#### 4.2.3. $CeO_2$ addition

$CeO_2$ addition to the MgO-supported palladium catalyst via the co-precipitation method results in a slightly lower yield compared to the PdO/n-MgO catalyst. The lower yield is not related to a decrease in Pd surface area as it is slightly higher on the CP PdO/$CeO_2$/n-MgO catalyst compared with the PdO/n-MgO catalyst without added $CeO_2$ (Table 3). However, this preparation method causes leaching of palladium into the reaction mixture, which is evident as a Pd mirror on the reaction flask wall after reaction. The palladium leaching indicates strong Pd–$CeO_2$ interactions during the co-precipitation which undermine the Pd interactions with the support. Leaching, in turn, lowers the activity despite a higher initial Pd surface area compared to the PdO/n-MgO catalyst without added $CeO_2$.

On the contrary, no palladium leaching was observed in the reactions using the SQ PdO/$CeO_2$/n-MgO catalyst. This catalyst has a higher Pd surface area than the co-precipitated catalyst, increases the product yield 17% over the PdO/n-MgO catalyst without added $CeO_2$, and increases the yield 60% over PdO supported on precalcined n-MgO. However, similar to the SQ PdO/$CeO_2$/n-$Al_2O_3$(+) catalyst, there appears to be a larger variation in yields compared to other catalysts. A catalyst prepared using the modified sequential precipitation method results in an even broader yield distribution and is thus not a very stable catalyst. It is possible that the catalytic activities of the n-MgO supported catalysts are very dependent on the drying and calcination procedure as $Mg(OH)_2$ decomposes to MgO beginning at 320 °C [38] and continues to decompose up to 800 °C (Fig. 2). The large variations in yields from these catalysts could be due to varying amounts of palladium leaching during reaction, which may be challenging to detect in some cases. It is also possible that $CeO_2$ migration over the Pd/PdO on the catalyst surface occurs during reaction contributing to lower than expected yields from the measured Pd surface area.

#### 4.2.4. $ZrO_2$ addition

Unlike the results for the n-$Al_2O_3$(+) support, adding $ZrO_2$ to the PdO/n-MgO catalyst yields a slightly lower activity for both preparation methods. This is despite the fact that both catalysts, CP and SQ, have higher Pd surface areas than the PdO/n-MgO catalyst without added $ZrO_2$. The CP catalyst gives slightly better average yields than the SQ catalyst, which is attributed to a higher Pd surface area since the turnover numbers are the same. As palladium leaching is observed in some runs using the CP PdO/$ZrO_2$/n-MgO catalyst, this can account for the lower activity compared with the reference PdO/n-MgO catalyst. For the SQ PdO/$ZrO_2$/n-MgO catalyst, both the yields and the measured Pd surface areas vary significantly between runs, indicating an unstable catalyst. Although the measured Pd surface areas are higher, the turnover numbers of the PdO/$ZrO_2$/n-MgO catalysts are lower in comparison to the PdO/n-MgO catalyst revealing less active catalysts.

The co-precipitation method is slightly better than the sequential precipitation method for n-MgO-supported catalysts due to removal of hydroxyl groups during the first calcination treatment. However, the preferred preparation method is dependent on the added oxide, as the sequential preparation method gives a higher yield for the PdO/$CeO_2$/n-MgO catalyst. Compared to the other catalysts under investigation, the BET surface areas of the n-MgO-supported catalysts are very low. The significant reduction in MgO surface area during catalyst preparation is not directly due to calcination of the support (Table 1). Instead the drastic reduction in surface area appears to originate during the palladium depo-

sition step. This may be attributed to partial dissolution of the MgO (or $Mg(OH)_2$) support in the slightly acidic $Pd(NO_3)_2$ (aq) solution [39]. $CeO_2$ addition increases the yield of the PdO/n-MgO catalyst, mainly due to an increased Pd surface area. However, a sequential precipitation method is necessary to prevent leaching of palladium.

### 4.3. PdO supported on nanoparticle titania

The n-$TiO_2$ has a very high surface area (~500 $m^2$/g), but the PdO/n-$TiO_2$ catalyst is only moderately active, comparable to the typical Pd/C in the oxidative coupling of 4-methylpyridine. Therefore, the addition of oxides with favorable properties has the highest potential for improving the catalytic performance of the catalysts under investigation. Moreover, the variation in yield of the PdO/n-$TiO_2$ catalyst has been shown to be larger than for PdO/n-$Al_2O_3$(+). Thus, the addition of ZnO, $CeO_2$ and $ZrO_2$ was investigated to determine if more reproducible and active catalysts can be obtained from n-$TiO_2$-supported PdO.

#### 4.3.1. Precalcination of n-$TiO_2$

Precalcination of the n-$TiO_2$ support before PdO deposition does not notably affect the yield of the resulting catalyst (Fig. 1). However, the measured Pd surface area is significantly lower on the precalcined n-$TiO_2$ support compared to the reference PdO/n-$TiO_2$ catalyst (Table 3), which is likely due to the drastic reduction in BET surface area with calcination of the n-$TiO_2$ support (Table 1). The heat treatment causes a 74% reduction in surface area, from 505 to 133 $m^2$/g, compared to a 59% reduction in Pd surface area observed on the calcined support. In contrast to the n-$Al_2O_3$(+) and n-MgO supports, the n-$TiO_2$ does not appear to contain a high number of hydroxyl groups. The TGA reveals a dry weight-loss of only 3.4% for the n-$TiO_2$ support with most of this weight-loss occurring before the 350 °C calcination temperature.

It appears that the drastic change in BET surface area with calcination of the n-$TiO_2$ support is due to a phase change (Fig. 5). The as received n-$TiO_2$ is nearly amorphous with an indication of an anatase phase present, but there is no significant long range order and the presence of other phases cannot be excluded. The XRD spectra of the PdO/n-$TiO_2$ catalyst clearly reveal the growth of anatase crystallites with calcination. Precalcination followed by another calcination treatment after palladium deposition likely increases the anatase phase contribution, as seen for the SQ PdO/$ZrO_2$/n-$TiO_2$ catalyst in Fig. 5. Anatase is known to result in strong Pd-support interactions [40] and has been shown to result in highly active PdO catalysts in the oxidative coupling of 4-methylpyridine [20]. Therefore, development of the anatase phase during calcination is likely the reason the lower Pd surface area on the precalcined support does not result in a reduction in yield.

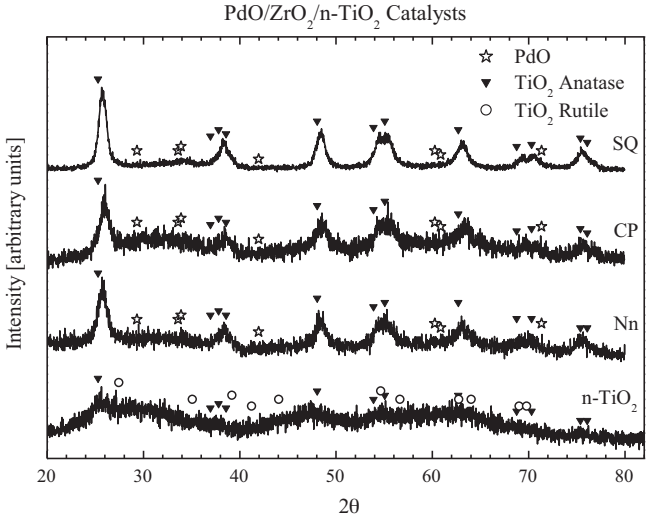


**Fig. 5.** X-ray diffraction (XRD) data obtained from PdO/$ZrO_2$/n-$TiO_2$ catalysts prepared using the co-precipitation (CP) and the sequential precipitation (SQ) methods, PdO/n-$TiO_2$ catalyst with no added $ZrO_2$ (Nn), and the n-$TiO_2$ support.

#### 4.3.2. ZnO addition

Similar to the behaviors of the n-$Al_2O_3$(+)- and n-MgO-supported catalysts, addition of ZnO results in lower yields than those obtained from the PdO/n-$TiO_2$ without ZnO. In this case, the sequential precipitation method produces a higher yield than the co-precipitation, the latter reducing the yield 31% compared to the n-$TiO_2$ without added ZnO. As for the other CP ZnO-containing catalysts, it appears that ZnO is covering the palladium on the CP PdO/ZnO/n-$TiO_2$ catalyst, as the overall surface area is larger, but the Pd surface area is lower compared to the PdO/n-$TiO_2$ catalyst. In contrast, on the SQ PdO/ZnO/n-$TiO_2$ catalyst the Pd surface area is larger than on the PdO/n-$TiO_2$ catalyst, but the yield is lower. It is likely that the presence of ZnO disrupts the favorable PdO-anatase $TiO_2$ interactions, either by simply blocking the n-$TiO_2$ from PdO or via the formation of a mixed oxide between ZnO and n-$TiO_2$ (such as $ZnTiO_4$ [41]).

#### 4.3.3. $CeO_2$ addition

$CeO_2$ addition to PdO/n-$TiO_2$ has minimal effect on the yield if sequentially precipitated and decreases the yield if co-precipitated onto the support with palladium. Similar to the behavior of CP PdO/$CeO_2$/n-MgO, the CP PdO/$CeO_2$/n-$TiO_2$ catalyst results in a significant amount of palladium leaching. Therefore, it appears that co-precipitation of Ce and Pd precursors on the n-MgO and n-$TiO_2$ supports weakens the Pd-support interactions. The Pd–Ce interactions are likely stronger than the Ce–Ti and Pd–Ti interactions [20,35,36,42]. Since leaching is not observed on the CP PdO/$CeO_2$/n-$Al_2O_3$(+) catalyst, this may indicate that the Pd interactions with the hydroxyl groups of AlO(OH) in the n-$Al_2O_3$(+) are stronger than the Pd–Ce interactions during deposition. For both the SQ and CP PdO/$CeO_2$/n-$TiO_2$ catalysts, addition of $CeO_2$ increases the amount of CO adsorbed on the catalysts compared to the PdO/n-$TiO_2$ without $CeO_2$, indicating that the Pd surface areas are larger for the $CeO_2$-containing catalysts. However, as the yields are not significantly higher, the turnover numbers are lower for the PdO/$CeO_2$/n-$TiO_2$ catalysts. While palladium leaching from the catalyst surface likely leads to lower than expected yields, it is also possible that $CeO_x$ species migrate over the palladium surface species thereby reducing the active metal surface area and the yield. This has been observed previously for PdO/$CeO_2$ catalysts [20].

#### 4.3.4. $ZrO_2$ addition

The sequentially precipitated PdO/$ZrO_2$/n-$TiO_2$ catalyst has a higher activity than the catalyst prepared using the co-precipitation method, which is similar to the behavior of the other n-$TiO_2$-supported catalysts (PdO/ZnO/n-$TiO_2$ and PdO/$CeO_2$/n-$TiO_2$). The SQ PdO/$ZrO_2$/n-$TiO_2$ catalyst results in a 20% higher yield, while the CP PdO/$ZrO_2$/n-$TiO_2$ catalyst yield is significantly lower in comparison to the PdO/n-$TiO_2$ catalyst. Table 3 reveals that the Pd surface areas are almost the same on the CP and SQ PdO/$ZrO_2$/n-$TiO_2$ catalysts and, thus, cannot account for the observed differences in activity. While leaching of palladium is common on the n-$TiO_2$ supported catalysts, it does not explain the low yield of the CP catalyst. It appears that palladium leaching affects the SQ PdO/$ZrO_2$/n-$TiO_2$ catalyst more than the CP PdO/$ZrO_2$/n-$TiO_2$ catalyst, as evidenced in a palladium mirror covering the reaction flask after completed reactions. Compared to the n-$Al_2O_3$(+) and n-MgO-supported catalysts, the product yields and Pd surface areas vary more for the n-$TiO_2$-supported catalysts, which indi-

cates these catalysts are not stable and/or are very sensitive to preparation conditions.

To further probe the differences between the SQ and CP $PdO/ZrO_2/n\text{-}TiO_2$ catalysts, they were subjected to XRD analysis (Fig. 5). A significantly higher contribution from the anatase phase is obsevered on the SQ $PdO/ZrO_2/n\text{-}TiO_2$ catalyst indicating the presence of larger anatase crystallites on this catalyst. The XRD spectra obtained from the CP $PdO/ZrO_2/n\text{-}TiO_2$ and the $PdO/n\text{-}TiO_2$ catalysts are very similar. While the two heat treatments could be the sole cause of the higher anatase contribution on the SQ $PdO/ZrO_2/n\text{-}TiO_2$ catalyst, the addition of $Zr^{4+}$ to $TiO_2$ possibly obstructs rutile phase formation and results in more anatase phase [43]. As the anatase phase has been shown to result in more favorable Pd–support interactions compared to other crystal phases or amorphous $TiO_2$ [40], the higher yield obtained from the SQ $PdO/ZrO_2/n\text{-}TiO_2$ catalyst is attributed to the increased anatase phase. In fact, the sequential precipitation method for all the $n\text{-}TiO_2$-supported catalysts is likely more active due to the increased anatase phase. As the activities of these catalysts are affected by the $n\text{-}TiO_2$ support crystal structure, and the amount of crystalline anatase phase is dependent on the calcinations, the $n\text{-}TiO_2$-supported catalysts are likely very sensitive to pretreatment conditions, such as calcination temperature and time. Since two calcinations at 350 °C result in more anatase phase, this indicates that the $n\text{-}TiO_2$ support is still changing after 3 h at this temperature. This can explain the reproducibility issues for these catalysts. Furthermore, the added $ZrO_2$ on these catalysts likely disrupts the favorable Pd–$TiO_2$ interactions resulting in an unstable catalyst where palladium leaches into the reaction solution and causes a reduction in yield despite the high palladium surface areas of the $PdO/ZrO_2/n\text{-}TiO_2$ catalysts.

In contrast to the $n\text{-}Al_2O_3(+)$-supported catalysts, the sequential preparation is the preferred method for the $n\text{-}TiO_2$-supported catalysts. This is likely due to an increased contribution from the anatase $TiO_2$ phase with calcination thus increasing favorable PdO–$TiO_2$ interactions. However, the addition of another oxide to the $PdO/n\text{-}TiO_2$ catalysts appears to disrupt the favorable Pd–$TiO_2$ interactions and leads to increased Pd leaching in several cases. Only $ZrO_2$ results in a significant increase in the yield obtained from $n\text{-}TiO_2$-supported PdO catalysts, if the catalyst is prepared using the sequential precipitation method. The effect of $ZrO_2$ is mainly to increase the Pd surface area, as the turnover numbers for the $PdO/n\text{-}TiO_2$ and $PdO/ZrO_2/n\text{-}TiO_2$ catalysts are very similar.

## 5. Conclusions

It is evident that there is no correlation between the measured Pd surface area and the catalytic activity over these catalysts. As the measured Pd particle size is reasonably consistent with the PdO particle sizes in the previous TEM results [20,31], it seems likely that the reaction is structure sensitive. However, migration of oxides to cover the active Pd species as well as palladium leaching also contribute to the lack of correlation with measured Pd surface area.

The optimal preparation method and the best additive to use for PdO catalysts in the oxidative coupling of 4-methylpyridine is dependent on the support used. In general, the co-precipitation method is favored for the $n\text{-}Al_2O_3(+)$ support, as the first calcination treatment removes support hydroxyl groups which are important to give a high Pd dispersion. The sequential precipitation yields better results for the $n\text{-}TiO_2$ support, since the heat treatment induces crystal growth of the anatase phase, which in turn leads to favorable PdO–support interactions. The n-MgO support is not as sensitive to heat treatment as the $n\text{-}Al_2O_3(+)$ support, so the best preparation method depends on the additive.

There are complex interactions between the PdO, the added oxide, and the nanoparticle oxide support in these catalysts. If the PdO–additive oxide interactions are too strong, they undermine the PdO–support interactions and lead to Pd leaching. If the PdO–support interactions are stronger, addition of another oxide is ineffective or reduces the PdO–support interactions leading to Pd leaching and a lower activity. Therefore, only a few $PdO/MeO_x/n\text{-support}$ catalysts are more active than the corresponding PdO/n-support catalyst.

As an additive, ZnO generally decreases the activity of the catalysts. This is accredited to strong ZnO–PdO interactions that either block active PdO sites or undermine the PdO–support interactions, or to strong ZnO–support interactions leading to mixed oxide formation, which reduces favorable ZnO–PdO and/or PdO–support interactions.

$CeO_2$ increases the Pd surface area of all catalysts and does promote the reaction in some cases. However, the yields obtained from $CeO_2$-containing catalysts vary significantly. Strong PdO–$CeO_2$ interactions resulting in disrupted PdO–support interactions and leaching of palladium and/or $CeO_x$ migration to cover active PdO species on the surface are identified as potential reasons for the reproducibility issues observed on these catalysts.

Addition of $ZrO_2$ also increases the Pd surface area on most catalysts. While $ZrO_2$ is a true promoter for the $PdO/n\text{-}Al_2O_3(+)$ catalyst, i.e. not only the yield but also the turnover number increase, this is not the case for the other supports. The yields obtained from the CP $PdO/ZrO_2/n\text{-}Al_2O_3(+)$ catalyst are consistently 36% higher at $3.4 \pm 0.1$ g product per g catalyst than the previously reported best yield in this reaction (2.5 g/g catalyst).

## Acknowledgements

Acknowledgment is made to the Donors of the American Chemical Society Petroleum Research Fund for support of this research.

XRD measurements were performed at the Major Analytical Instrumentation Center (MAIC) at the University of Florida. The MAIC director, Dr. Amelia Dempere, is gratefully acknowledged for the support of this research. The authors are also thankful for the advice and instruction of Dr. Valentin Craciun.

The BET and TGA data were collected at the Particle Engineering Research Center at the University of Florida. The authors are grateful for the training on the BET machine provided by Mr. Gill Brubaker and on the TGA instrument by Mr. Nate Stevens.

## References

[1] R.C. Evans, P. Douglas, C.J. Winscom, Coord. Chem. Rev. 250 (2006) 2093.
[2] C. Kaes, A. Katz, M.W. Hosseini, Chem. Rev. 100 (2000) 3553.
[3] U.S. Schubert, C. Eschbaumer, Angew. Chem. Int. Ed. 41 (2002) 2892.
[4] V. Balzani, A. Juris, M. Venturi, S. Campagna, S. Serroni, Chem. Rev. 96 (1996) 759.
[5] V. Balzani, G. Bergamini, F. Marchioni, P. Ceroni, Coord. Chem. Rev. 250 (2006) 1254.
[6] C.D. Clark, M.Z. Hoffman, Coord. Chem. Rev. 159 (1997) 359.
[7] L. Gámiz-Gracia, A.M. Garcıía-Campaña, J.J. Soto-Chinchilla, J.F. Huertas-Pérez, A. González-Casado, Trends Anal. Chem. 24 (2005) 927.
[8] N.M.L. Hansen, K. Jankova, S. Hvilsted, Eur. Polym. J. 43 (2007) 255.
[9] D.L. Feldheim, C.J. Baldy, P. Sebring, S.M. Hendrickson, C.M. Elliott, J. Electrochem. Soc. 142 (1995) 3366.
[10] H. Ishii, M. Goyal, M. Ueda, K. Takeuchi, M. Asai, Appl. Catal. A 201 (2000) 101.
[11] F. Tsai, B. Lin, M. Chen, C. Mou, S. Liu, Tetrahedron 63 (2007) 4304.
[12] W. Wu, S. Chen, F. Tsai, Tetrahedron Lett. 47 (2006) 9267.
[13] 4,4′-Dimethyl 2,2′-bipyridine, GFS Chemicals: http://gfschemicals.com/statics/productdetails/cHJvZHVjdGRldGFpbHMxMjc=.html, accessed 12/15/2010.
[14] H. Hagelin, B. Hedman, I. Orabona, T. Åkermark, B. Åkermark, C.A. Klug, J. Mol. Catal. A 164 (2000) 137.
[15] P.K. Ghosh, T.G. Spiro, J. Am. Chem. Soc. 102 (1980) 5543.
[16] P.A. Adcock, F.R. Keene, R.S. Smythe, M.R. Snow, Inorg. Chem. 23 (1984) 2336.

[17] G. Sprintschnik, H.W. Sprintschnik, P.P. Kirsch, D.G. Whitten, J. Am. Chem. Soc. 99 (1977) 4947.
[18] L.M. Neal, H.E. Hagelin-Weaver, J. Mol. Catal. A 284 (2008) 141.
[19] L.M. Neal, D. Hernandez, H.E. Hagelin-Weaver, J. Mol. Catal. A 307 (2009) 29.
[20] L.M. Neal, M.L. Everett, G.B. Hoflund, H.E. Hagelin-Weaver, J. Mol. Catal. A 335 (2011) 210.
[21] C.E. Gigola, M.S. Moreno, I. Costilla, M.D. Sanchez, Appl. Surf. Sci. 254 (2007) 325.
[22] W. Shen, Y. Matsumura, J. Mol. Catal. A 153 (2000) 165.
[23] J. Kaspar, P. Fornasiero, M. Graziani, Catal. Today 50 (1999) 285.
[24] J.M. Padilla, G. Del Angel, J. Navarrete, Catal. Today 133–135 (2008) 541.
[25] A. Trovarelli, C. de Leitenburg, M. Boaro, G. Dolcetti, Catal. Today 50 (1999) 353.
[26] R. Zhou, B. Zhao, B. Yue, Appl. Surf. Sci. 254 (2008) 4701.
[27] L.M. Martinez, T.C. Montes de Correa, J.A. Odriozola, M.A. Centeno, Catal. Today 107–108 (2005) 800.
[28] L. Bollmann, J.L. Ratts, A.M. Joshi, J. Catal. 257 (2008) 43.
[29] G.R. Newkome, A.K. Patri, E. Holder, U.S. Schubert, Eur. J. Org. Chem. (2004) 235.
[30] S. Liu, K. Takahashi, H. Eguchi, K. Uematsu, Catal. Today 129 (2007) 287.
[31] L.M. Neal, S.D. Jones, M.L. Everett, G.B. Hoflund, H.E. Hagelin-Weaver, J. Mol. Catal. A 325 (2010) 25.
[32] NanoScale Corporation http://www.nanoscalecorp.com/content.php/chemicals/powders/, accessed on 11/19/2010. n-$Al_2O_3$(+): NanoActive Aluminum Oxide Plus, n-MgO: NanoActive Magnesium Oxide Plus, and n-$TiO_2$: NanoActive Titanium Dioxide.
[33] B. Didillon, E. Merlen, T. Pagès, D. Uzio, Stud. Surf. Sci. Catal. 118 (1998) 41.
[34] S.D. Jones, L.M. Neal, H.E. Hagelin-Weaver, Appl. Catal. B 84 (2008) 631.
[35] A. Badri, C. Binet, J.C. Lavalley, J. Chem. Soc., Faraday Trans. 92 (1996) 1603.
[36] S. Naito, T. Kasahara, T. Miyao, Catal. Today 74 (2002) 201.
[37] R.N. Gayen, S.N. Das, S. Dalui, R. Bhar, A.K. Pal, J. Crystal Growth 310 (2008) 4073.
[38] K. Itatani, K. Koizumi, F. Scott Howell, A. Kishioka, M. Kinoshita, J. Mater. Sci. 23 (1998) 3405.
[39] D.R. Lide (Ed.), CRC Handbook of Chemistry and Physics, 90th ed., CRC Press Taylor & Francis Group, Boca Raton, FL, 2010, pp. 8–137.
[40] Y. Li, Y. Fan, H. Yang, B. Xu, L. Feng, M. Yang, Y. Chen, Chem. Phys. Lett. 372 (2003) 160.
[41] C.T. Wang, J.C. Lin, Appl. Surf. Sci. 254 (2008) 4500.
[42] H. Zhu, Z. Qin, W. Shan, W. Shen, J. Wang, J. Catal. 225 (2004) 267.
[43] N. Venkatachalam, M. Palanichamy, B. Arabindoo, V. Murugesan, J. Mol. Catal. A 266 (2007) 158.